Grain Growth in Open Systems

GUSAK Andriy[1, a *], KOZUBSKI Rafal[2,b] and TYSHCHENKO Dmytro[3,c]

[1]Department of Physics, Cherkasy National University, Ukraine

[2]Department of Physics, Jagellonian University, Cracow, Poland

[3]Department of Physics, Cherkasy National University, Ukraine

[a]amgusak@ukr.net, [b]rafal.kozubski@uj.edu.pl, [c]kwazar2008@ukr.net

Abstract. Grain growth in open systems is analyzed for the cases of flux-driven ripening during soldering, flux-driven lateral growth during deposition of thin films, flux-driven lateral growth during reactive growth of intermediate phase, flux-driven lateral growth of antiphase domains in FCC-phase A3B and BCC-phase AB during the diffusion growth of ordered phase layer.

1. Introduction

Most of solid materials are polycrystalline. Evolution of their structure means, first of all, the change of grain size and grain shape distributions. This problem is commonly known as the Grain Growth problem. Usually, grain growth means coarsening, i.e. the growth of mean grain size. The problem of grain growth is one of the traditional fields of the materials science [1-10]. In this paper we will concentrate on the non-traditional aspect of this traditional problem, the grain growth in open systems. Here, under open system we will imply (1) diffusion zone of the diffusion couple, (2) thin film under various deposition conditions, and (3) reaction zone during solid state reaction. In all the mentioned cases the new material is produced in the system. This material is typically poly-, or even nanocrystalline, and demonstrates the coarsening. This coarsening, as we will see below, is very different from the coarsening in closed systems due to fluxes of matter through the open system. Below we present a few examples of coarsening in open systems: (1) Flux Driven Ripening in reaction between solid copper or nickel with tin-based molten solder, (2) Flux-Driven Grain Growth during deposition of a thin film on the inert substrate (theory, model and special experiment), (3) Flux-Driven Coarsening of grains of the growing intermediate layer during reactive diffusion – elementary estimations, (4) Flux-Driven Coarsening of antiphase domains in ordered intermediate phase layers (A3B in the case of FCC lattice and AB in the case of BCC lattice).

2. Basic Aspects of Flux-Driven Ripening

The growth of intermetallic compound Cu_6Sn_5 (or Ni_3Sn_4) during reactions between Cu (or Ni) and molten tin-based solder is accompanied with diffusion coarsening. A classical coarsening stage in closed systems typically starts after the growth stage when the total volume of a new phase almost reaches an asymptotic maximal volume, and this volume is now just redistributed among competing grains [11-13]. The driving force of classical coarsening in closed system is the reduction of surface energy due to the reduction of interface surface area. Contrary to this, reactions between molten solder and metal demonstrate that ripening of scallop-type intermetallic phase in the contact zone proceeds simultaneously with scallop growth. Since the volume of intermediate phase increases with time, this type of coarsening can be called non-conservative. The driving force of this process is the release of free energy due to the production of intermetallic phase volume.

If one assumes scallops to have a hemispherical shape, then the total area of an interface is just twice larger than the planar cross-section area ($A^{\text{interface}} \approx \sum 2\pi R_i^2 = 2\sum \pi R_i^2 \approx 2A^{\text{cross section}}$) and therefore is not changing with time in the process of growth. The scallop growth is observed during

the reaction between eutectic SnPb solder and Cu and also between Pb-free solders (for example, SnAg) and Cu, and between pure tin and copper [14-19]. It was experimentally shown that as the layers of reaction products grow, the scallops ripening takes place, and the corresponding model describing this phenomenon was proposed as well. In [20-21] the new kinetic theory was developed for the new type of coarsening (jointly with King Ning Tu), based on (a) conservation of the interface area at increasing volume and (b) dominating role of channels between the scallops. This phenomenon was called flux-driven ripening (FDR).

Soldering (using the tin-based solders) proceeds at about 200°C-250°C, the typical time of soldering being from a few seconds to several minutes. The result of soldering reaction is the formation of intermetallic compounds Cu_3Sn and Cu_6Sn_5. In case of reaction with molten solder the Cu_6Sn_5 is the dominant growth phase (due to fast penetration of copper through the liquid channels) and has scallop-type morphology. The size of the scallops can grow to several microns in diameter after a few minutes of reaction at 200°C-250°C between molten solder and Cu. The mean radius of scallops grows with time approximately as $t^{1/3}$. The number of scallops decreases with time as $t^{-2/3}$. On the other hand, the Cu_3Sn is a thin layer and its growth is very slow. Liquid channels between the scallops remain during the whole process. The morphology of scallops and channels, most probably, is thermodynamically stable under the presence of molten solder. Indeed, the molten eutectic solder SnPb quickly wets the grain boundaries of Cu_6Sn_5. These channels are actually the fast diffusion paths supplying copper to the molten solder. Then extra copper precipitates at the scallops enabling their growth. The channel width will be theoretically evaluated in the next Section.

3. Attempt of Evaluation of the Channel Width in FDR.

As mentioned above, the formation of the scallop-like η-phase during the reaction of copper substrate with the liquid tin-based solder proceeds much faster than the same phase growth in the reaction with solid solder under the temperature just a little lower than the eutectic one. It cannot be related to the temperature dependence of diffusion in intermetallic compound. Instead, it is related to the easy-diffusion paths emerging between the neighboring scallops, which let copper intensively diffuse into the melt and there to react with tin at the scallop/liquid interfaces. To the best of our knowledge, there are 3 ways of interpreting the easy-diffusion paths in the mentioned system:

1. According to [20-21], the paths are just liquid channels formed due to full wetting of inter-scallop boundaries by liquid solder, so that grain-boundary tension between two neighboring grains of compound is larger than two interface tensions between the scallop and liquid solder: $\gamma_{\eta\eta} > 2\gamma_{\eta/l}$ (*). In this case the liquid channels are formed towards the very bottom of scallops – towards the copper substrate (at first) and later towards the layer of ε-phase Cu3Sn1.

2. According to [22], the wetting of grain-boundaries by the liquid solder is not full: $\gamma_{\eta\eta} < 2\gamma_{\eta/l}$ (**). In this case the easy paths are the grooved grain boundaries between scallops.

3. There is also a compromise possibility [23]: the scallops growing at the base of the same copper grain have close orientations, so that grain boundaries between them have low tension, and condition (**) is satisfied. On the other hand, the scallops growing at different (neighboring) grains, have large misorientations, grain-boundaries between them have high tension, they are wetted by liquid solder, and condition (*) is satisfied.

Cases (1) and (3) mean the existence of the liquid channels. Let us make some theoretical predictions for the width of channels [24]. Obviously, it cannot be too big, since there is a driving force of reaction which will lead to filling the existing gap by the η-phase growing grains. On the other hand, it cannot be zero because then two compound/liquid interfaces will convert into one grain-boundary between two solid grains, then the energy will increase due to condition (*).

Let us consider the channel of some width δ dividing two parallel walls of η-compound grains based on the substrate of ε-phase. In this configuration the bottom of the channel presents the

contact of liquid tin-based solution and ε-phase, so that in usual free contact one might expect emergence of η-phase. Yet, in our case it should mean simultaneously the change of surface energy. It means that we actually have the nucleation problem – competition of bulk and surface terms. The only peculiarity is that the nucleus now is the island of η-phase containing grain-boundary instead of two preexisting η-phase/liquid interfaces.

Nucleation can be "homogeneous" ("kissing" of grains somewhere at arbitrary point contact of two walls – disk of η-phase) and "heterogeneous" – emerging of η-phase island (semi-cylindrical or rectangular "sheet" of η-phase) at the base of ε-phase bottom. The second possibility seems to be more probable due to the presence of copper necessary to form a "sheet" of η-phase from the tin-based liquid.

For simplicity consider a semi-disc of radius R and thickness δ at the bottom of the channel. The semi-disc consists of two semi-discs of some thicknesses δ_1, δ_2, $\delta_1 + \delta_2 = \delta$ being the "continuations" of the two neighboring grains. An exact position of a grain-boundary (and the related δ_1 / δ_2 ratio) does not influence the energy and therefore is not important.

The change of Gibbs free energy due to the formation of a semi-disc is equal to

$$\Delta G\left(R, \delta\right) = \left(-\frac{\Delta g_{\varepsilon+solder \to \eta}}{\Omega}\right) \cdot \delta \cdot \frac{1}{2} \pi R^2 + \left(\gamma_{\eta/\eta} - 2\gamma_{\eta/liquid}\right) \cdot \frac{1}{2} \pi R^2$$
$$+\gamma_{\eta/liquid} \cdot \pi R \cdot \delta + \left(\gamma_{\eta/\varepsilon} - \gamma_{\varepsilon/liquid}\right) \cdot 2R \cdot \delta$$

$$(1)$$

The first term is a "bulk" one. The second term corresponds to the change from two solid/liquid interfaces to one grain-boundary. The third term corresponds to a side semicircle. The last, fourth term, corresponds to the change of the bottom rectangular side interface from liquid/epsilon to eta/epsilon.

As usual in nucleation problems, let us unite terms with squared radius and with linear radius:

$$\Delta G\left(R, \delta\right) = \left(\gamma_{\eta/\eta} - 2\gamma_{\eta/liquid} - \frac{\Delta g_{\varepsilon+solder \to \eta}}{\Omega} \delta\right) \cdot \frac{1}{2} \pi R^2$$
$$+\left(\frac{\pi}{2}\gamma_{\eta/liquid} + \gamma_{\eta/\varepsilon} - \gamma_{\varepsilon/liquid}\right) \cdot \delta \cdot 2R$$

$$(2)$$

One can easily see that the R-dependence of Gibbs free energy (1) can have typical barrier type at

$$\delta > \frac{\gamma_{\eta/\eta} - 2\gamma_{\eta/liquid}}{\Delta g_{\varepsilon+solder \to \eta}} \Omega$$

or (2) can be monotonically increasing at

$$\delta < \frac{\gamma_{\eta/\eta} - 2\gamma_{\eta/liquid}}{\Delta g_{\varepsilon+solder \to \eta}} \Omega.$$

Thus, there exists some "critical" channel width, under which the further filling of the liquid channel by eta-phase is impossible.

$$\delta^* = \frac{\gamma_{\eta/\eta} - 2\gamma_{\eta/liquid}}{\Delta g_{\varepsilon+solder \to \eta}} \Omega$$

$$(3)$$

If $\delta > \delta^*$, then the nucleation is not even needed, and the channel will proceed becoming narrower by normal movement of walls till the width reaches the mentioned critical value.

4. Basic Equations of FDR

Let $f(t, R)$ be the scallop radii distribution function (under the assumption of hemispherical scallops). Since all scallops are based on the same substrate with fixed total area, S^{total}, their total volume grows but the sum of their basement areas remains almost constant. The constraint of constant interface is:

$$\sum_{i=1}^{N} \pi R_i^2 = \int_0^\infty \pi R^2 f(t, R) dR = S^{total} - S^{free} \cong S^{total} = const.$$ (4)

In Eq. (4) we neglected the area S^{free} of channels cross-section. It determines the incoming flux of copper into the molten solder and is approximately equal to

$$S^{free} = \int_0^\infty \frac{\delta}{2} 2\pi R f(t, R) dR.$$ (5)

The volume of the growing intermetallic scallop is

$$V_i = \sum_{i=1}^{N} \frac{2}{3} \pi R_i^3 = \int_0^\infty \frac{2}{3} \pi R^3 f(t, R) dR.$$ (6)

The major constraint of our system is the conservation of mass. Namely, if molten solder is saturated with copper (and the saturation is reached fast in a small micro-bump), then the 'in-flux' of copper is fully consumed by growing intermetallic scallops. It means that the product of the in-flux density J^{in} of copper and of the channels cross-section area S^{free} is equal to the increase of copper quantity in the growing volume of the intermediate phase.

$$n_i C_i \frac{dV_i}{dt} = J^{in} S^{free}.$$ (7)

Here n_i, C_i are atomic density and mole fraction of copper in the growing intermetallic, respectively. The 'in-flux' density is determined by Fick's law with average gradient being equal to the ratio of the difference $\Delta C = C^b - C^e$ (between the equilibrium concentrations of copper in solder with substrate and with growing scallops of intermetallic phase), and average width of the reaction zone (approximately equal to average radius of a grain):

$$J^{in} \cong -nD \frac{C^e - C^b}{<R>}.$$ (8)

Since scallops must grow and shrink atom by atom, the distribution function should satisfy the usual continuity equation in the size space:

$$\frac{\partial f}{\partial t} = -\frac{\partial}{\partial R}(f u_R),$$ (9)

where the velocity in the size space, u_R, is just the growth rate of scallops found from the equation for the flux density:

$$u_R = \frac{dR}{dt} \cong \frac{-j(R)}{n_i C_i}.$$ (10)

Flux in (out) of each individual scallop is proportional to the difference between the mean-field chemical potential of copper μ in the reaction zone and the chemical potential $\mu_\infty + \dfrac{\beta}{R}$ at the spherical scallop-melt surface:

$$j(R) = -L\left(\mu - \mu_\infty - \frac{\beta}{R}\right).$$ (11)

Here the parameters L, μ are determined self-consistently from the above mentioned two constraints – of constant surface and mass conservation.

Equations (4) – (11) lead to the following equation for distribution function:

$$\frac{\partial f}{\partial t} = -\frac{k}{9} \frac{<R>}{<R^2>-<R>^2} \frac{\partial}{\partial R}\left(f\left(\frac{1}{<R>}-\frac{1}{R}\right)\right),$$ (12)

where the growth rate k is determined by the incoming flux conditions instead of the surface tension (contrary to LSW-theory of ripening in a closed system):

$$k = \frac{9}{2}\frac{n}{n_i}\frac{D(C^b-C^e)\delta}{C_i}$$ (13)

The mean cubed radius is proportional to time:

$$<R^3> = kt.$$ (14)

The normalized size distribution function is

$$g(u) = 0.0169\frac{u}{(2-u)^4}\exp\left(-\frac{4}{2-u}\right), \quad u = R/<R>.$$ (15)

Thus, the mean size kinetics is the "LSW-like" (LSW: Lifshitz-Slezov-Wagner [11-13]) and size distribution is "Hillert-like" [2] demonstrating that FDR incorporates the features both of ripening and of grain growth.

5. Basic Aspects of Flux-Driven Grain Growth during Deposition

In 2003 Tu, Gusak and Sobchenko generalized the idea of grain growth in an open system on the case of thin film deposition. The model was called the Flux-Driven Grain Growth (FDGG) [25].

(a)   (b)
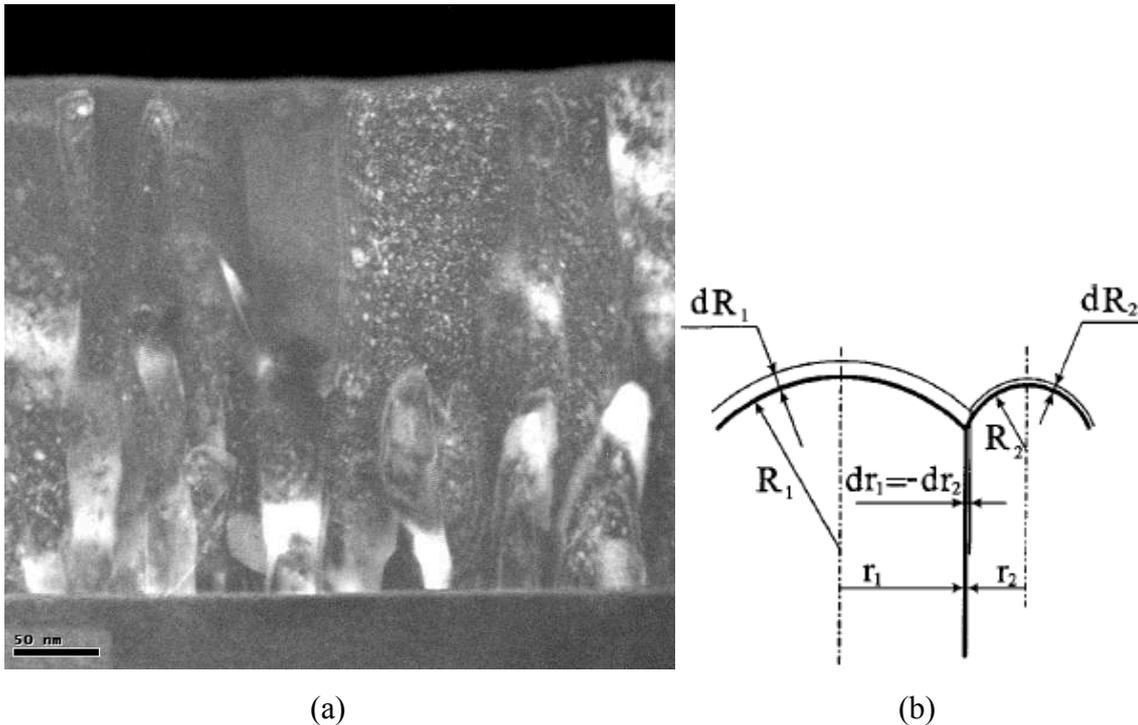
Fig 1. (a) Cross-sectional view of grain structure after the 250-nm Al film deposition at room temperature (Zeiss Libra 200 FE, dark-field mode) [26];
(b) Idea and basic scheme of "mushroom" effect

We considered the grain growth simultaneously with the formation of bamboo structure during the thin film deposition (Fig.1). The main idea was the so-called mushroom (edge) effect – the grain structure of a new atomic layer is basically inherited from the previous layer, but can slightly differ

from the previous in a very narrow band (of atomic thickness 2δ) just above the grain boundary. If an ad-atom is about to become attached in this region, it can choose between the two adjacent grains as host. In order to obtain the linear growth law, the authors assumed in [25] that the above mentioned choice is done in a deterministic way, i.e. an atom which lands within the 2δ-band always chooses the larger grain as its host. So, the larger grain extends in each new deposited layer and gradually overlaps the neighboring smaller grain. This scheme has led to the conclusion that the average lateral diameter should develop according to the relationship $2\overline{R} \approx 0.8 \cdot (\delta/d) \cdot h$ in which d denotes the inter-planar distance.

In [26], an experiment with Al deposition demonstrated that the growth of the lateral mean size is substantially slower and, moreover, it is better approximated by the parabolic dependence. Thus, a revision of the FDGG model was required. It turned out that thermodynamic probabilities had to be taken into account when the choice of the host grain is made: The probability is controlled by the local curvature $1/r$ of a grain boundary, which generates the difference of pressure between both sides of the boundary $\Delta p = \gamma/r$ (the Laplace pressure/tension, depending on curvature sign). Hence, the difference of binding enthalpy exists, $\Delta H = \Omega\Delta p = \gamma\Omega/r$. Therefore, the probabilities of

sticking to one of the adjacent grains are equal to $e^{\pm\frac{\gamma\Omega}{2rkT}} / \left[e^{\frac{\gamma\Omega}{2rkT}} + e^{-\frac{\gamma\Omega}{2rkT}} \right]$, so that the local lateral

shift of the grain boundary after the deposition of a new atomic layer of thickness d will amount to

$$< \Delta x >= \delta \cdot \tanh\left(\frac{\gamma\Omega}{2rkT}\right). \tag{16}$$

Accordingly, the velocity of lateral grain boundary motion is given by

$$v = \frac{<\Delta x>}{\Delta t_{layer}} = \frac{<\Delta x>}{\left(d/(dh/dt)\right)} = \frac{dh}{dt}\frac{\delta}{d} \cdot \tanh\left(\frac{\gamma\Omega}{2kT}\frac{1}{r}\right). \tag{17}$$

If the ratio $\gamma\Omega/(kTr)$ is large, the previous FDGG model is retained with $v = \pm\frac{dh}{dt}\frac{\delta}{d}$

depending on the curvature direction. However, if the ratio $\gamma\Omega/(kTr)$ is small enough (e.g. $r = 20nm, \gamma = 0.5 \ J/m^2, \Omega = 2 \cdot 10^{-29} m^3, T = 300K$ yield a ratio of $0.12 \ll 1$), the function may be approximated by its argument. In this case, the migration velocity of the grain boundary becomes proportional to its local curvature, as has been used before in the Neuman-Mullins approach for conventional thermal grain growth in the 2D case [4, 5]:

$$v = M\frac{\gamma}{r} \text{ with } M = \frac{dh}{dt} \cdot \frac{\delta}{d} \cdot \frac{\Omega}{2kT}. \tag{18}$$

As has been shown in numerous previous works on conventional grain growth, such dependence of the driving force always leads to a parabolic growth law for the mean size, as in the case of conventional grain growth. The only but fundamental difference in the case of FDGG is that the effective lateral mobility M is proportional to the deposition rate, while it is determined by the kinetics of the detachment of atoms from one grain structure and incorporation into another in the case of conventional grain growth. Thus, one may formulate:

$$\overline{R}^2 - \overline{R}_0^2 = k \cdot t = \kappa \cdot h, \tag{19}$$

where

$$\kappa = \frac{k}{dh/dt} = p \cdot \frac{M\gamma}{dh/dt}. \tag{20}$$

6. Attempt of FDGG-Theory for the Case of Reactive Diffusion

Here we will compare the kinetics of common normal grain growth with lateral grain growth in the growing phase layer during reactive diffusion.

At first, we will evaluate the lateral grain growth rate in a closed thin film. Very roughly, we will consider the film with bamboo structure and will treat each grain as approximately cylindrical (with some lateral radius and some height equal to the film thickness). The velocity of a grain boundary between two grains of lateral radii R_i and R_j (the velocity projection on the direction from grain i to grain j) can be estimated according to main principles of non-equilibrium thermodynamics with the account of the Laplace tension terms:

$$\upsilon = -L\frac{\Delta\mu}{\delta} \approx -\frac{D^{\perp *}}{kT}\frac{1}{\delta}\left(p_i^{Lapl}\Omega - p_j^{Lapl}\Omega\right) \approx -\frac{D^{\perp *}}{kT}\frac{1}{\delta}\left(\frac{\gamma\Omega}{R_i} - \frac{\gamma\Omega}{R_j}\right). \tag{21}$$

Here $\Delta\mu$ is a difference of chemical potentials between the neighboring grains due to their different sizes; L is the Onsager coefficient, proportional to the tracer diffusion coefficient $D^{*\perp}$ across the boundary; p_i^{Lapl} is the Laplace pressure within the i-th grain, δ is the grain boundary width and γ is the grain boundary tension.

Then the rate of the i-th grain radius change is approximately equal to

$$\frac{dR_i}{dt} \sim -\frac{D^{\perp *}}{kT}\frac{1}{\delta}\left(\frac{\gamma\Omega}{R_i} - \frac{\gamma\Omega}{R}\right), \tag{22}$$

where R is the mean lateral grain radius.

Then the rate of the mean radius growth is approximately equal (as shown in the Hillert's model of normal growth [2]) to

$$\left.\frac{dR}{dt}\right|^{normal} \sim \kappa\frac{D^{\perp *}}{kT}\frac{1}{\delta}\frac{\gamma\Omega}{R}, \tag{23}$$

where κ is about one (more close to 0.5).

Now we will estimate the lateral diffusion induced growth rate in an open system. We see this process in the following way: atom A in the process of the reactive diffusion migrates (at relatively low temperature) through the layer of ordered intermediate phase along the grain boundary or along the boundary between the anti-phase domains. Time τ of this migration will be estimated below. At the end of the travel along the boundary the atom should react with B and join one of grains or one of antiphase domains. By the joining the atom continues the intermediate phase grain (domain) both in lateral direction as well as in the direction of intermediate layer growth. The choice of a grain (domain) to join is determined by the difference of probabilities

$$\Delta p = \left(\exp\left(-\frac{\gamma\Omega}{kTR_i}\right) - \exp\left(-\frac{\gamma\Omega}{kTR_j}\right)\right) \Big/ \left(\exp\left(-\frac{\gamma\Omega}{kTR_i}\right) + \exp\left(-\frac{\gamma\Omega}{kTR_j}\right)\right) \approx \frac{\gamma\Omega}{2kT}\left(\frac{1}{R_j} - \frac{1}{R_i}\right), \tag{24}$$

The average lateral displacement from grain i toward grain j is determined by the product of these probabilities difference and of the interatomic distance:

$$\Delta x_{i\to j} \approx a\frac{\gamma\Omega}{2kT}\left(\frac{1}{R_j} - \frac{1}{R_i}\right). \tag{25}$$

Hence, the rate of the grain lateral growth (or shrinking) approximately equals to

$$\frac{dR_i}{dt} \approx \frac{a}{\tau}\frac{\gamma\Omega}{2kT}\left(\frac{1}{R} - \frac{1}{R_i}\right). \tag{26}$$

Then the rate of the mean radius growth due to distribution of "newly arrived" atoms among domains (grains) is equal to

$$\left.\frac{dR}{dt}\right|^{FDGG} \approx \kappa \frac{a}{\tau} \frac{\gamma\Omega}{2kT} \frac{1}{R} . \tag{27}$$

Here τ is the time of migration across the phase layer along the grain boundary (along the boundary between domains). Let us estimate this time. The effective flux density through the phase layer of thickness h equals to

$$\bar{J}_B = \frac{1}{\Omega} C_i \bar{V} \approx \frac{1}{\Omega} \frac{\delta}{R} D_{GB}^{*//} \frac{\Delta g}{kT} \frac{1}{h}, \tag{28}$$

where Δg is the thermodynamic driving force of phase formation.

Thus, the mean velocity $\bar{V}$ of atoms B migration through the phase layer is

$$\bar{V} \approx \frac{1}{C_i} \frac{\delta}{R} D_{GB}^{*//} \frac{\Delta g}{kT} \frac{1}{h} . \tag{29}$$

Here $D_{GB}^{*//}$ - is the tracer diffusivity along the grain boundary.

Thus, the average time spent by atoms during the travel along the boundary is

$$\tau = \frac{h}{\bar{V}} \approx h^2 R \frac{kTC_i}{\delta D_{GB}^{*//}\Delta g} . \tag{30}$$

Hence, for the lateral grain growth in an open system one gets:

$$\left.\frac{dR}{dt}\right|^{FDGG} \approx \kappa \frac{a}{\tau} \frac{\gamma\Omega}{2kT} \frac{1}{R} = \kappa \frac{a}{\left(h^2 R \dfrac{kTC_i}{\delta D_{GB}^{*//}\Delta g}\right)} \frac{\gamma\Omega}{2kT} \frac{1}{R} . \tag{31}$$

Now we find the ratio of the lateral growth rates in open and closed systems:

$$\left.\frac{dR}{dt}\right|^{FDGG} \approx \kappa \frac{a}{\tau} \frac{\gamma\Omega}{2kT} \frac{1}{R} = \kappa \frac{a}{\left(h^2 R \dfrac{kTC_i}{\delta D_{GB}^{*//}\Delta g}\right)} \frac{\gamma\Omega}{2kT} \frac{1}{R} \qquad \left.\frac{dR}{dt}\right|^{normal} \sim \kappa \frac{D^{\perp *}}{kT} \frac{1}{\delta} \frac{\gamma\Omega}{R} . \tag{32}$$

$$\frac{dR/dt|^{FDGG}}{dR/dt|^{normal}} = \frac{\kappa \dfrac{a}{\left(h^2 R \dfrac{kTC_i}{\delta D_{GB}^{*//}\Delta g}\right)} \dfrac{\gamma\Omega}{2kT} \dfrac{1}{R}}{\kappa \dfrac{D^{\perp *}}{kT} \dfrac{1}{\delta} \dfrac{\gamma\Omega}{R}} = \frac{a\delta^2}{2C_i R h^2} \frac{\Delta g}{kT} \frac{D_{GB}^{*//}}{D_{GB}^{*\perp}} . \tag{33}$$

Thus, the ratio of grain growth rates in open and in closed polycrystalline layer depends on its thickness, as well as on the mean grain size, changing with time. The thinner is layer, the stronger should be influence of external fluxes on the lateral grain growth.

7. Model Monte Carlo Experiment for Polycrystalline A3B (FCC lattice) – Simultaneous Growth of Phase Layer Thickness and of Mean Lateral Grain Size Growth in Reactive Diffusion between A and AB

We tried to check our ideas of the previous section by Monte-Carlo modeling of domain growth in the ordered phase. We treat the anti-phase domains as grains and boundaries between the anti-phase domains as grain boundaries between grains with different orientations. Of course, we keep in mind that merging of domains is much more probable than merging of grains due to the much smaller set of possible domains than the set of possible orientations. We limit ourselves here by the exchange mechanism in the FCC lattice. The choice of pair energies was the following:

$$\Phi_{AA}/kT = -3, \Phi_{AB}/kT = -5, \ \Phi_{BB}/kT = -2.25 .$$

We compare the evolution kinetics for two cases. Case (1) – Closed system with elongated grains along axis Z (actually, 4 times a lattice parameter with periodic boundary conditions; note that one lattice parameter is equal to two inter-planar 001 distances) and 2D-coarsening in XY-plane. Case (2) – Open system – thin layer of intermediate ordered phase A3B (containing initial set of 4 types of competing anti-phase domains) between pure A and ordered AB phase.

The initial thickness of the intermediate ordered A3B layer was 3 times a lattice parameter; the initial thickness of AB marginal sample was 5 times a lattice parameter; and the initial thickness of pure A sample was also 5 times a lattice parameter, (A-A3B-AB-A3B -A…).

I. At first we tried to use the standard Residence Time Algorithm (RTA) for simulation of atomic migration both in closed and open systems. Namely, we assume that the activation barrier Q for each atomic exchange is constant, so that the magnitude of the saddle-point E^{saddle} is equal to $E^{saddle} = \dfrac{E^{old} + E^{new}}{2} + Q$. Then the energy needed to reach the saddle-point from the old state is $E^{saddle} - E^{old} = \dfrac{E^{new} - E^{old}}{2} + Q$. Then the probability of each possible exchange can be found as

$$p(i) = \frac{v_0 \exp\left(-\dfrac{E^{new}(i) - E^{old}(i)}{2kT}\right)}{\sum\limits_{j} v_0 \exp\left(-\dfrac{E^{new}(j) - E^{old}(j)}{2kT}\right)}. \tag{34}$$

The actual exchange is chosen among all possibilities for all possible exchanges of all atoms, and the time is added according to:

$$t := t + \frac{1}{\sum\limits_{j} v_0 \exp\left(-\dfrac{Q}{kT}\right) \exp\left(-\dfrac{E^{new}(j) - E^{old}(j)}{2kT}\right)}. \tag{35}$$

Here the sum is taken over all possible exchanges of all atoms with their nearest neighbors of alternative sort.

The "time" at the abscissa in Fig. 2 is actually

$$t^{reduced} := 10^3 \cdot t \cdot v_0 \exp\left(-\frac{Q}{kT}\right) \tag{36}$$

The ordinate in Fig. 2 is a mean number of atoms per a cross-section of a domain satisfying the condition of the ordered phase.

One can see that the growth in the open system is faster.

The initial decrease of lateral size in this computer experiment and in all experiments below is, evidently, due to the widening of the initially sharp boundaries between the antiphase domains. (We artificially prepared the set of ideally ordered antiphase domains. After the start of simulation, the domains start to lose the ideal order and the boundaries widen.)

(a)

(b)
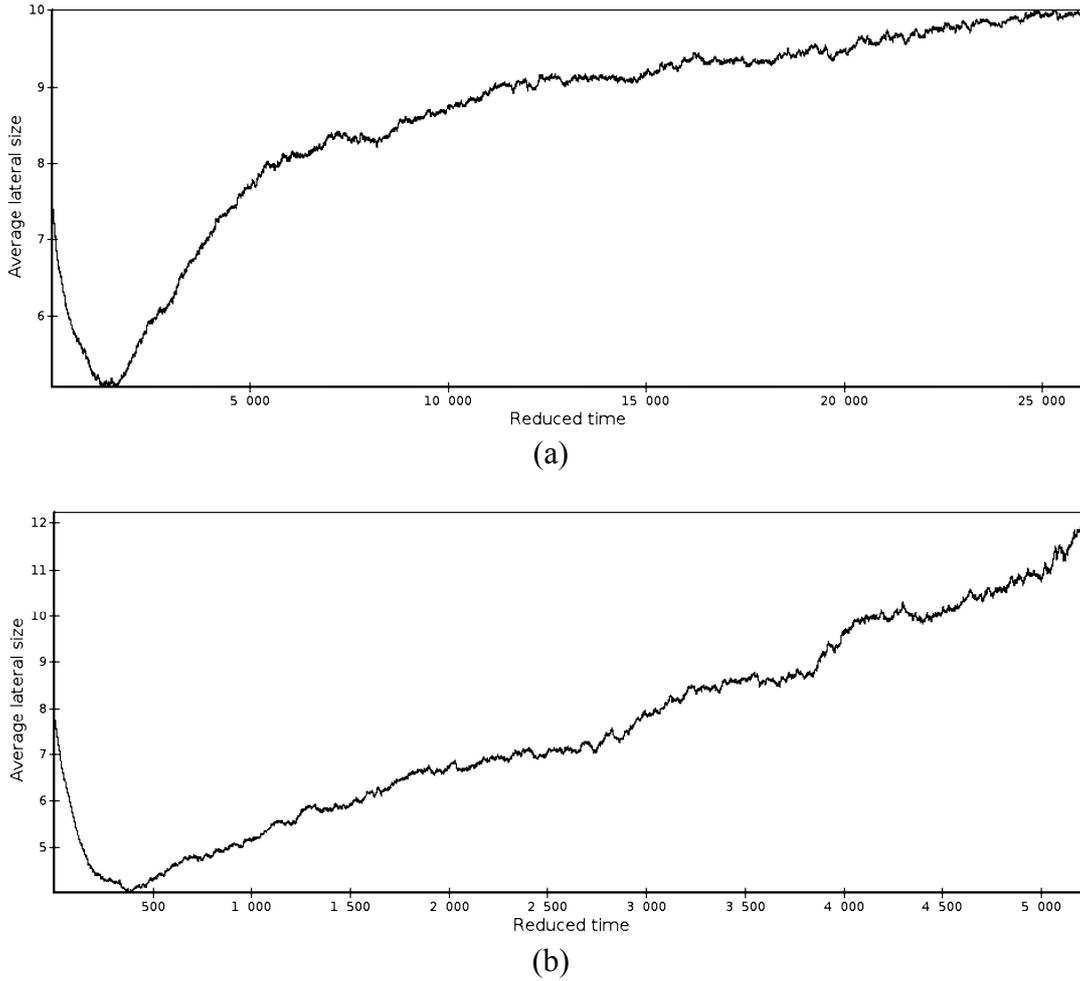
Fig. 2. Comparison of coarsening kinetics in closed (a) and open (b) systems at the RTA algorithm,

$$Q = \text{const}, \quad t^{reduced} := 10^3 \cdot t \cdot v_0 \exp\left(-\frac{Q}{kT}\right).$$

II. An alternative version of the algorithm is also well known. Let us assume that instead of Q the position of the saddle point, E^{saddle}, is common for all possible exchanges. Then the probability of the i-th exchange is given by

$$p(i) = \frac{v_0 \exp\left(-\frac{E^{saddle} - E^{old}(i)}{kT}\right)}{\sum_j v_0 \exp\left(-\frac{E^{saddle} - E^{old}(i)}{kT}\right)}. \tag{37}$$

$$t := t + \frac{1}{\sum_j v_0 \exp\left(-\frac{E^{saddle} - E^{old}(j)}{kT}\right)}. \tag{38}$$

Here the sum is taken over all possible exchanges of all atoms with their nearest neighbors of alternative sort.

The "time" at the abscissa in Fig. 3(a and b) is actually

$$t^{reduced} := 10^{-35} \cdot t \cdot v_0 \exp\left(-\frac{E^{saddle}}{kT}\right).$$
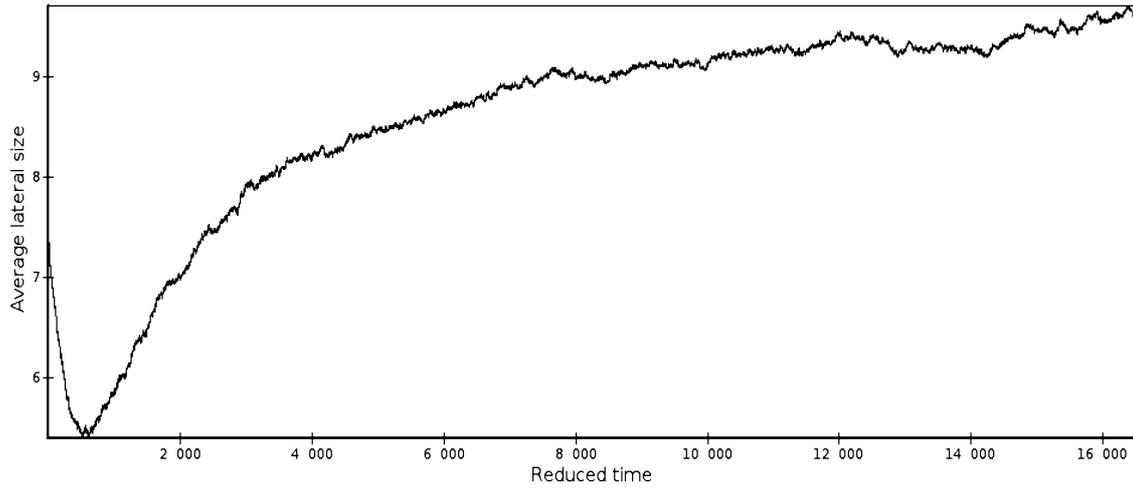
(a)
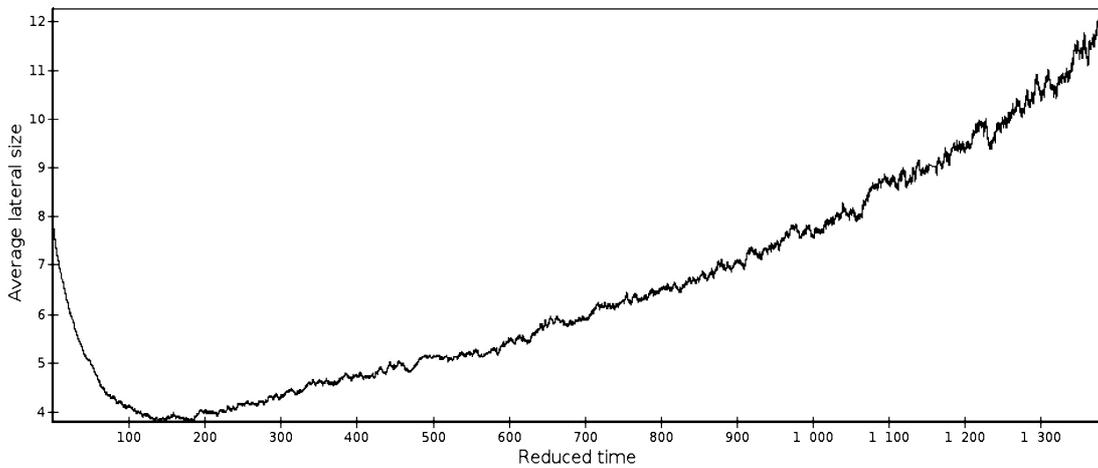
(b)

Fig. 3. Comparison of coarsening kinetics in closed (a) and open (b) systems at the RTA algorithm,

$$E^{saddle} = const \; , \; t^{reduced} := 10^{-35} \cdot t \cdot v_0 \exp\left(-\frac{E^{saddle}}{kT} \right).$$

In this case the growth in open system is faster as well.

III. Metropolis algorithm.

We tried one more version of algorithm – the most "ancient" one – the Metropolis algorithm. We randomly choose an atom and one of its neighbors. If the exchange leads to the decrease of energy, then the change is accepted, otherwise it is tried according to Boltzmann distribution. The exchange is not accepted if the randomly generated number from interval (0.1) is larger than $\exp\left(-\dfrac{E^{new} - E^{old}}{kT} \right)$.

One can see that the growth in open system under the Metropolis algorithm is also faster.

(a)

(b)
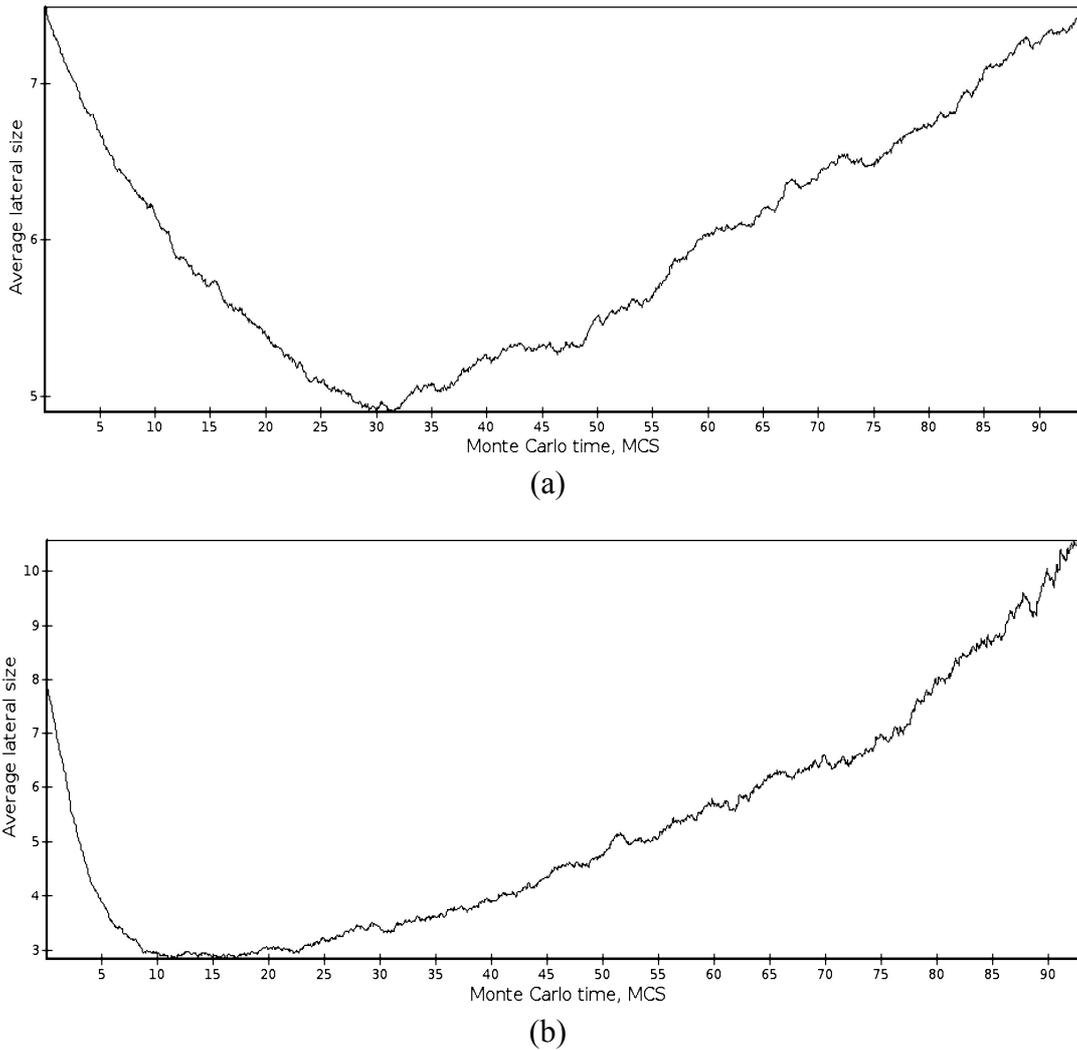
Fig. 4. Comparison of coarsening kinetics in closed (a) and open (b) systems at the Metropolis algorithm

8. Model Monte Carlo experiment – Thickness Growth and Simultaneous Lateral Grain Growth of Polycrystalline AB (BCC lattice) in Reactive Diffusion between A and B

Here we study the second-order transition in the open system with concentration gradient and corresponding fluxes. In this case of ordering at BCC lattice the choice of antiphase domains is of course more limited, namely, only two sublattices are available. Therefore the probability of simple merging is higher.

Open system: 7 times a lattice parameter for A, 5 times a lattice parameter for the initial AB couple at the rigid BCC lattice and 7 times a lattice parameter for B, (A-AB-B-AB-A…).

Similar to Section 7, we started with the standard Residence Time Algorithm. The probabilities and time scale are determined by Eqs. (34, 35).

The "time" at the abscissa in Figs. 5a,b is actually $t^{reduced} := 10^5 \cdot t \cdot \nu_0 \exp\left(-\dfrac{Q}{kT}\right)$.

(a)

(b)
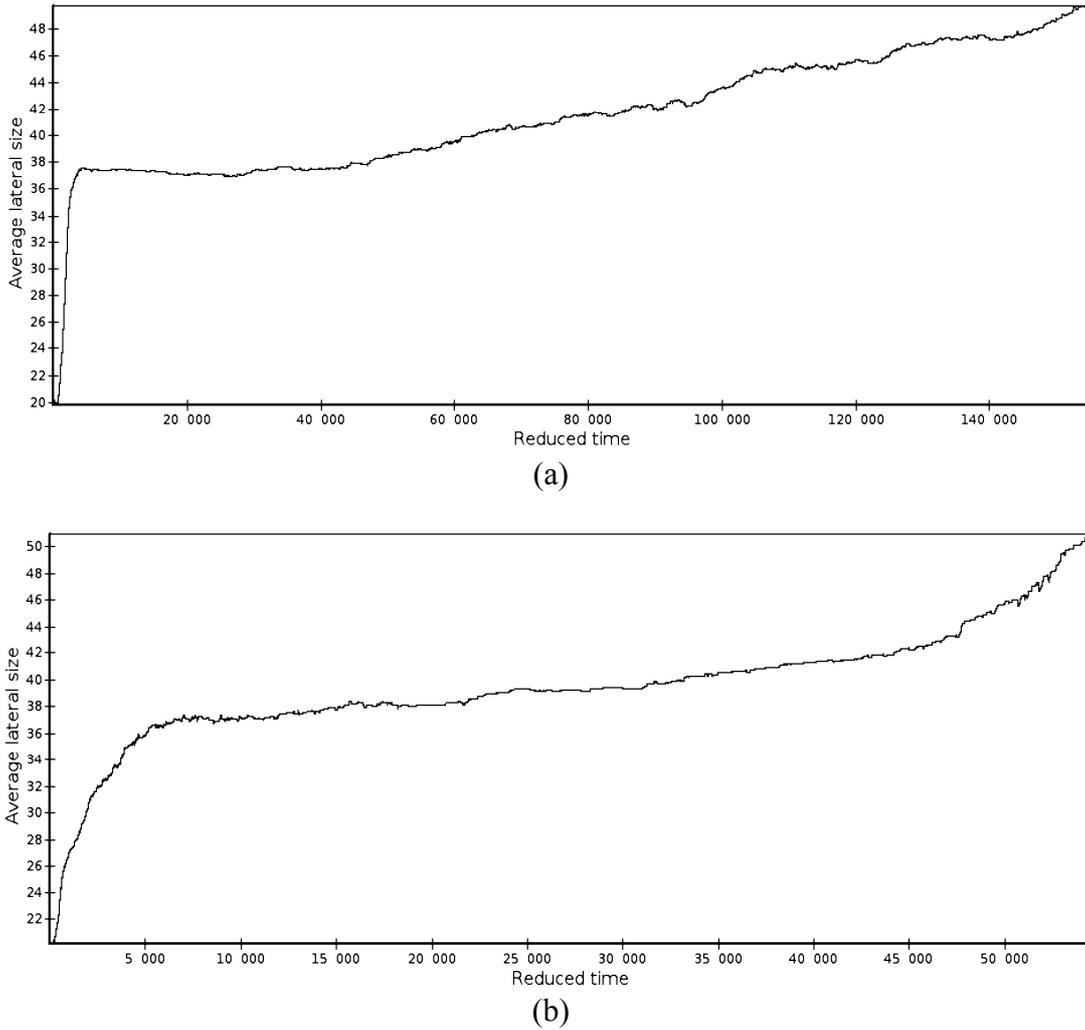
Fig. 5. Comparison of coarsening kinetics of the BCC AB phase in closed system (a) and in open system (b) at the RTA algorithm, Q=const, $t^{reduced} := 10^3 \cdot t \cdot \nu_0 \exp\left(-\dfrac{Q}{kT}\right)$.

Similar to the FCC-lattice, for the ordering in the BCC lattice we also tried the second version of the algorithm, with fixed saddle-point instead of fixed barrier height, according to Eqs. (37-38). In this case the "time" at the abscissa in Figs. 6a,b is actually

$$t^{reduced} := 10^{-19} \cdot t \cdot \nu_0 \exp\left(-\frac{E^{saddle}}{kT}\right).$$

Once more one can see the faster growth in the open system.

(a)

(b)
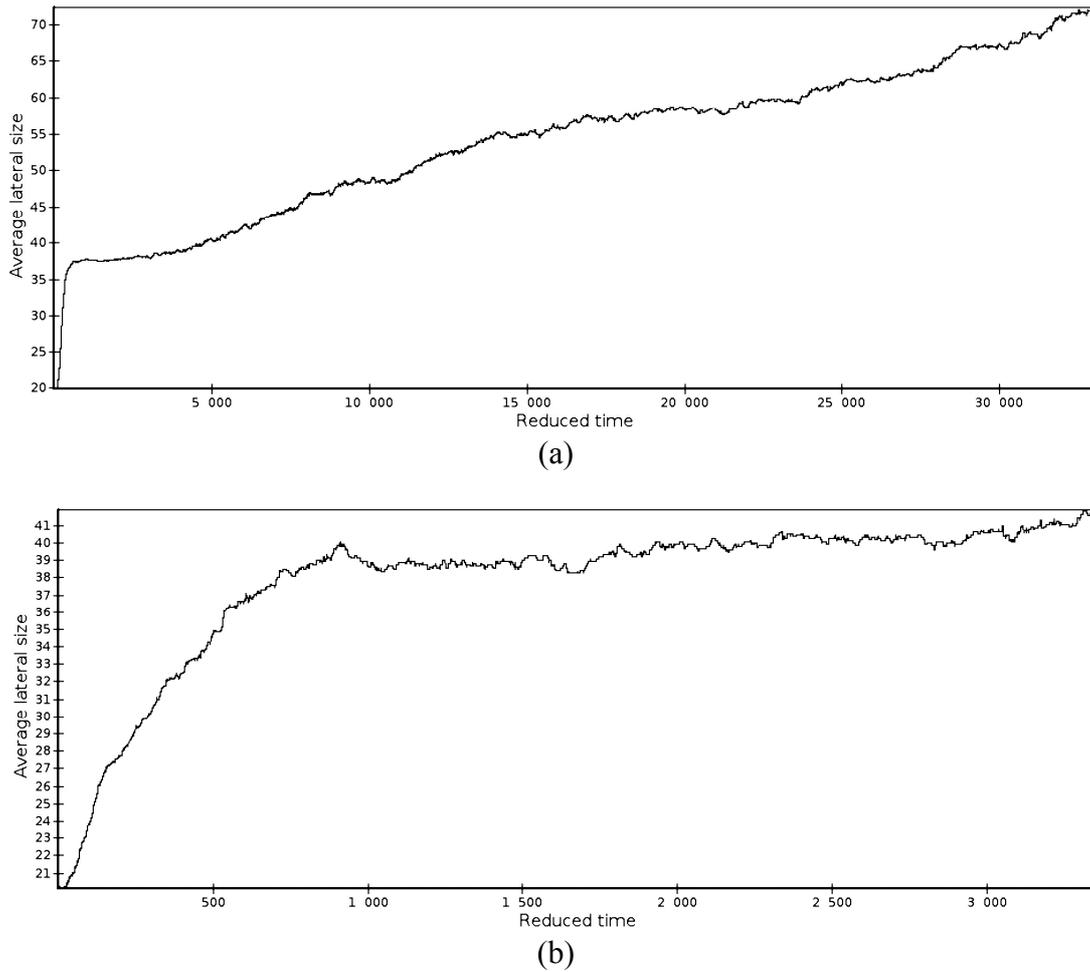
Fig. 6. Comparison of coarsening kinetics in BCC AB phase in closed system (a) and in open system (b) at RTA algorithm, $E^{saddle} = const$, $t^{reduced} := 10^{-19} \cdot t \cdot v_0 \exp\left(-\dfrac{E^{saddle}}{kT}\right)$.

Summary

1. The lateral grain growth during solid - liquid interactions in soldering proceeds due to external fluxes penetrating the reaction zone via the liquid channels, and the rate of the lateral grain growth is determined by 1/3 time law and is proportional to the channel width instead of surface tension, contrary to normal grain growth in closed thin films.

2. The lateral grain growth during the deposition can proceed due to the choice of host grain by the atoms arriving to the grain boundary junction from the vapor phase. Its rate is determined by the deposition rate.

3. The lateral grain growth during solid – solid interaction with the formation of intermediate phase layer can proceed due to the choice of host grain by the atoms arriving to the grain boundary junction through the growing phase layer.

4. The lateral growth of anti-phase domains during the reactive growth of A3B FCC-phase and of AB BCC phase proceeds faster in the open system than in the closed one. We are not ready to claim anything numerically at the moment but the faster grain growth in open systems seems evident. More accurate evaluation of the rates and of time scales will be reported elsewhere.

References

[1] J.E. Burke, D.R. Turnbull, Recrystallization and grain growth, Progr. Met. Phys. 3 (1952) 220-292.

[2] M. Hillert, On the theory of normal and abnormal grain growth, Acta. Metall. 13 (1965) 227-238.

[3] V.E. Fradkov, D.G. Udler, L.S. Shvindlerman, Computer simulation of grain growth in two dimensions, Scripta Metall. 19 (1985) 1285-1290.

[4] V.E. Fradkov, L.S. Shvindlerman, D.G. Udler, Short-range order in the arrangement of grains in two-dimensional polycrystals, Phil. Mag. Lett. 55 (1987) 289-294.

[5] M. Marder, Soap bubble growth, Phys. Rev. A 36 (1987) 438-440.

[6] P.E. Di Nunzio, A discrete approach to grain growth based on pair interactions, Acta Mater. 49 (2001) 3635-3643.

[7] N.P. Louat, On the theory of normal grain growth, Acta Metall. 22 (1974) 721-724.

[8] C.S. Pande, On a stochastic theory of grain growth, Acta Metall. 35 (1987) 2671-2678.

[9] C.V. Thompson, Grain Growth and Evolution of Other Cellular Structures, Solid State Physics, Academic Press 55 (2000) 269-314.

[10] A.M. Gusak, K.N. Tu, Theory of normal grain growth in normalized size space, Acta Mater. 51 (2003) 3895-3904.

[11] J.M. Lifshitz, V.V. Slezov, J. Phys. and Chem. Sol. 19 (1961) 35-50.

[12] C. Wagner, Theory of precipitate change by redissolution, Z. Electrochem. 65 (1961) 581-591.

[13] V.V. Slezov, Theory of diffusive decomposition of solid solutions, Harwood Academic, Dordrecht, 1995.

[14] R.A. Gagliano, M.E. Fine, Growth of η phase scallops and whiskers in liquid tin-solid copper reaction couples, JOM 53(6) (2001) 33-38.

[15] F. Bartels, J.W. Morris, Jr.G. Dalke, and W. Gust, Intermetallic phase formation in thin solid-liquid diffusion couples, J. Electron. Mater. 23 (1994) 787-790.

[16] H.K. Kim, K.N. Tu, Kinetic analysis of the soldering reaction between eutectic SnPb alloy and Cu accompanied by ripening, Phys. Rev. B 53 (1996) 16027-16034.

[17] K.N. Tu, K. Zeng, Tin-lead (SnPb) solder reaction in flip chip technology, Mater. Sci. Eng. Reports R34 (2001) 1-58.

[18] K.N. Tu, Fiona Ku, T.Y. Lee, Morphology stability of solder reaction products in flip chip technology, J. Electron. Mater. 30 (2001) 1129-1132.

[19] J.H. Lee, J.H. Park, Y.H. Lee, Y.S. Kim, and D.H. Shin, Stability of channels at a scalloplike Cu_6Sn_5 layer in solder interconnections, J. Mater. Res. 16 (2001) 1227-1230.

[20] A.M. Gusak, K.N. Tu, Kinetic theory of flux-driven ripening, Phys. Rev. B 66 (2002) 115403-1-14.

[21] K.N. Tu, A.M. Gusak, M. Li, Physics and materials challenges for lead-free solders, J. Appl. Phys. 93 (2003) 1335-1353.

[22] J. Gorlich, G. Schmitz, K.N. Tu, On the mechanism of the binary Cu/Sn solder reaction, Appl. Phys. Lett. 86 (2005) 053106-1-3.

[23] Jong-ook Suh, K.N. Tu, G.V. Lutsenko, A.M. Gusak, Size distribution and morphology of Cu6Sn5 scallops in wetting reaction between molten solder and copper, Acta Mater. 56 (2008) 1075-1083.

[24] A.M. Gusak, O.Yu. Liashenko, F. Hodaj, Models of phase formation, growth and competition in soldering - some new results, Bulletin of Cherkasy University 269 (2013) 3-18.

[25] K.N. Tu, A.M. Gusak, I. Sobchenko, Linear rate of grain growth in thin films during deposition, Phys. Rev. B 67 (2003) 245408-1-5.

[26] I. Sobchenko, G. Schmitz, A. Gusak, D. Baither, Proc. DIFTRANS-2007, Bulletin of Cherkasy University 117 (2007) 51-57.